Inverse Kinematics of a Reclaimer: Closed-Form Solution by Exploiting Geometric Constraints

Keum-Shik Hong*, Young-Min Kim** and Chintai Choi***

Inverse Kinematics of a Reclaimer: Closed-Form Solution by Exploiting Geometric Constraints

Keum-Shik Hong*, Young-Min Kim** and Chintai Choi***

(*Received October 10, 1996*)

The inverse kinematics of a reclaimer that excavates and transports raw materials in a raw yard is investigated. Because of the geometric feature of the equipment, in which scooping buckets are attached around a rotating disk, kinematic redundancy occurs in determining the joint variables. Link coordinates are introduced following the Denavit-Hartenberg representation. For a given excavation point the forward kinematics yields 3 equations in 4 variables. It is shown that the rotating disk at the end of the boom provides an extra passive degree of freedom. Two approaches are investigated in obtaining an inverse kinematics solution. The first method pre-assigns the height of the excavation point, which can be determined through path planning. A closed-form solution is obtained for the first approach. The second method exploits the orthogonality between the normal vector at an excavation point and the z-axis of the end -effector coordinate system. The geometry near the reclaiming point has been approximated as a plane, and the plane equation has been obtained by a least-squares method from 8 adjacent points near the point. A closed-form solution is not found for the second approach; however, a linear approximate solution is provided.

Key Words : Inverse Kinematics, Redundant Manipulator, Passive Degree of Freedom, Geometric Constraint, Normal Equation.

1. Introduction

The reclaimer is a type of industrial equipment that excavates and transports raw materials like coal and iron ore in the raw yard of a steel company. It can be classified as a type of a serial manipulator. The reclaimer consists of a main body, a boom and a tilted rotating drum. The boom is about 50 m long, and can rotate horizontally and vertically, while the main body moves on the rectilinear rail in the raw yard. The reclaimer consists of a rotating circular disk with

---

* Research Institute of Mechanical Technology, Pusan National University, 30 Changjeon -dong, Kumjeong-ku, Pusan 609-735, Korea Tel. +82−51−510−2454, Fax. +82−51− 514−0685,
Email : kshong@hyowon. pusan. ac. kr
** Graduate College, Pusan National University
*** Research Institute of Industrial Science and Technology, P. O. Box 135, Pohang 790-600

buckets attached to the circumference. The circular disk tilts at various angles so that the raw materials in the buckets can fall on the conveyor belt located in the middle part of the boom as the buckets rotate. Currently all the information about the type, quantity, and location of the raw materials to be transferred from the stockyard are communicated to an operator and the operator manually drives a reclaimer to the spot and excavates manually. Therefore, in the event of poor visibility or at night, it is difficult for the reclaimer to approach a desired spot on an ore pile.

In this paper the inverse kinematics problem of finding joint variables for a desired end-effector location is investigated. To the best of the authors knowledge no published results for the inverse kinematics problem of a reclaimer or other related subjects are yet to be found in the literature.

The first step toward automatic transmission of raw materials from the raw yard to a blast furnace

is to obtain the 3-dimensional information of a materials heap. This is achieved by scanning the heap with a laser sensor. With the examination of the degrees of freedom of the reclaimer mechanism, link coordinates are defined in terms of the Denavit-Hartenberg(D-H) representation. For a given excavation point the forward kinematics provides 3 equations; however, the number of joint variables in the equations is 4. Hence there exists one kinematic redundancy in the mechanism, and it will be shown that one passive degree of freedom occurs from the rotating disk at the end of boom. In the paper the inverse kinematics problem is viewed in two different ways. One is to find a solution for a given excavation point in space, and the other is to find a solution for a given end-effector's location and orientation in space. The first approach does not include the information of the surrounding environment in the problem formulation. Kinematic redundancy exists in the 4 DOF mechanism. The excavation point needs to be determined by considering how to eliminate all the raw materials from the ground rather than by attempting to answer the kinematic redundancy in the mechanism itself. Hence the first approach utilizes the fact that the drum height during slewing can be decided beforehand through path planning. The second approach exploits a geometric constraint such that the circle connecting the tips of the buckets should contact the surface of the raw materials heap. Hence, regarding the rotating disk as a rigid body in space, the problem becomes to position a rigid body for a given position and orientation in space. In this case the manipulator should have at least 6 joints to provide general 6 DOF motion in space. However, the reclaimer has only 4 DOF. A closed-form solution is obtained for the first method; however, a closed-form solution to the second approach is not available. Instead a linear approximation of the solution to the second approach is proposed.

The contributions of the paper are as follows. First, the authors are almost sure that the study in the paper is the first and only systematic discussion on a reclaimer to appear in the literature. No single conference or journal paper has been found

yet. Secondly, the closed-form inverse kinematics solution obtained through path planning has been proven reliable by experiments and has been implemented in the stockyards of Pohang Steel Company, Ltd., in Korea. The paper has the following structure. The degrees of freedom of the reclaimer is investigated in Sec. 2. In Sec. 3 the reference and link coordinates are defined by using the D-H representation, and the forward kinematics equations are derived. Section 4 investigates a closed-form solution for the inverse kinematics problem which involves obtaining joint variables with the assumption that the height of slew level of the boom is given through path planning. Section 5 investigates the inverse kinematics problem for an arbitrary landing point. Two approaches are compared in Sec. 6 and conclusions are given in Sec. 7.

2. Degree of Freedom

The degrees of freedom (DOF) of a mechanism is the number of independent inputs or parameters required to determine the locations of all the points in the mechanism. We investigate the DOF of the reclaimer with the following schematic diagram in Fig. 1.

The rectilinear motion of the main body moving on a rail is simplified as a prismatic joint ①, and the two rotational motions of the boom are simplified as revolute joints ② and ③, respectively. It is also shown that the rotating disk at the end of the boom is connected by a revolute joint . Therefore, the number of inputs to represent an arbitrary point P' on the circumference of the disk is obtained by the following equation (Sandor and Erdman, 1984):
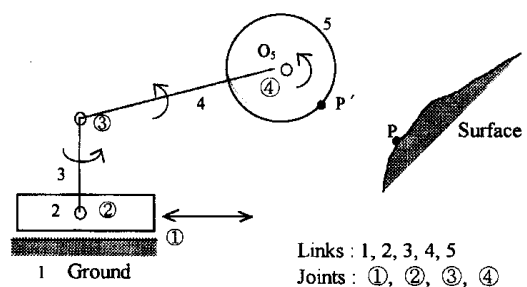

Fig. 1   Reclaimer and its schematic diagram

$$F = \lambda(l - j - 1) + \sum_{i=1}^{i} f_i \qquad (1)$$

where F=DOF of a mechanism, l=number of links, j=number of joints, f_i=DOF of the ith joint, λ=DOF that the mechanism can have in space.

In the case of the reclaimer l=5, j=4 (1 prismatic and 3 revolute joints). Since each joint can have only one degree of freedom, $\sum f_i$ = 4. λ=6 due to the spatial motion of the mechanism. Therefore, the degrees of freedom of the reclaimer F=4 is obtained.

The necessity of finding the point P' on the circumference of link 5 becomes clearer from the fact that the location of the point P on a raw materials heap determines P'. However, once P' contacts P, F becomes 0 which means that there is no mobility in the mechanism, here the contact point P has been considered as a two DOF joint.

Now we examine the input-output relation of the mechanism. The 3-dimensional coordinates of

point P', (x_0, y_0, z_0), becomes the output. One rectilinear displacement of joint ① and two rotational displacements of joints ② and ③ are the inputs. Normally three independent inputs can determine the location of a point in space; however, in the case of the reclaimer there exists an extra link 5 and it provides an extra passive degree of freedom in the mechanism.

3. Coordinate Systems

Figure 2 shows the reference and link coordinate systems of the reclaimer using the D-H representation (Fu et al., 1987). Varying parameters are written in italic and constant parameters are written in normal face in the Table of Fig. 2. The 1st link coordinate is attached to the main body which moves on the rail. The 2nd and 3rd link coordinates indicate that the boom can rotate with the angles θ_2 and θ_3, respectively. The 4th and 5th link coordinates indicate that the rotating disk tilts at the angles of φ and ψ,
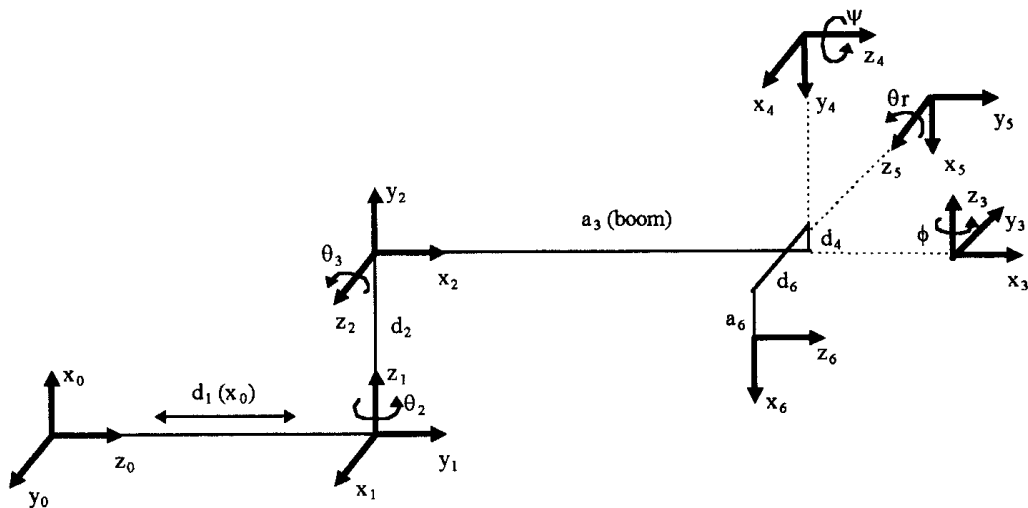
i	a_i	α_i	d_i	θ_i
1	0	$\pi/2$	d_1	$\pi/2$
2	0	$\pi/2$	d_2	$\pi/2 + \theta_2$
3	a_3	$-\pi/2$	0	θ_3
4	0	$-\pi/2$	d_4	$-\pi/2 + \varphi$
5	0	$\pi/2$	0	$\pi/2 + \psi$
6	a_6	$-\pi/2$	d_6	θ_r

Fig. 2 Establishing link-coordinate systems and its parameters

respectively. θ_r denotes the angle from the x_5 axis to the x_6 axis about the z_5 axis.

For a desired excavation point $(x_0,\ y_0,\ z_0)$ in the reference coordinate system, the forward kinematics provides 3 equations as follows:

$$x_0 = \sin\ \theta_3\{\ a_6\cos\ \phi\sin\ \theta_r + \sin\ \phi(\mathrm{d}_6\cos\ \psi$$
$$-\ a_6\sin\ \psi\cos\theta_r)\ \}$$
$$+\cos\ \theta_3(-\ a_6\cos\ \psi\cos\ \theta_r - \mathrm{d}_6$$
$$\sin\ \psi + \mathrm{d}_4) + a_3\sin\ \theta_3 + \mathrm{d}_2 \qquad (2)$$

$$y_0 = -\sin\ \theta_2[\cos\ \theta_3\{\ a_6\cos\ \phi\sin\ \theta_r$$
$$+\sin\ \phi(\mathrm{d}_6\cos\ \psi - a_6\sin\ \psi\cos\ \theta_r)\ \}$$
$$-\sin\ \theta_3(-\ a_6\cos\ \psi\cos\ \theta_r - \mathrm{d}_6$$
$$\sin\ \psi + \mathrm{d}_4) + a_3\cos\ \theta_3]$$
$$+\cos\ \theta_2\{\ \cos\ \phi(\mathrm{d}_6\cos\ \psi - a_6\sin\ \phi$$
$$\cos\ \theta_r) - a_6\sin\ \phi\sin\ \theta_r\ \} \qquad (3)$$

$$z_0 = \cos\ \theta_2[\cos\ \theta_3\{\ a_6\cos\ \phi\sin\ \theta_r$$
$$+\sin\ \phi(\mathrm{d}_6\cos\ \psi - a_6\sin\ \psi\cos\ \theta_r)\ \}$$
$$-\sin\ \theta_3(-\ a_6\cos\ \psi\cos\ \theta_r - \mathrm{d}_6\sin\ \psi$$
$$+\mathrm{d}_4) + a_3\cos\ \theta_3]$$
$$+\sin\ \theta_2\{\ \cos\ \phi(\mathrm{d}_6\cos\ \psi - a_6\sin\ \psi\cos$$
$$\theta_r) - a_6\sin\ \phi\sin\ \theta_r\ \} + d_1 \qquad (4)$$

In Eqs. (2) ~ (4) the varying joint parameters are d_1, θ_2, θ_3 and θ_r. Therefore there exists one extra degree of freedom in determining the joint variables. The existence of an extra degree of freedom can also be seen in Fig. 3, which indicates infinitely many circles passing through a point if the disk is contacting the surface of the bulk.
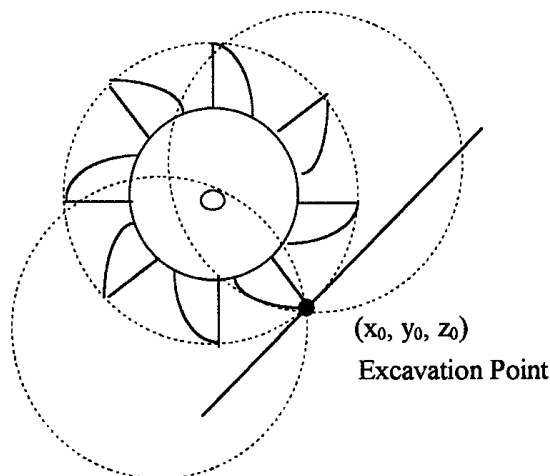

Fig. 3 Infinitely many circles passing through an excavation point

4. Inverse Kinematics (Approach #1)

In this section we investigate the inverse kinematics problem when the drum height is pre-assigned while slewing of the boom occurs. This approach focuses on how the entire materials can be eliminated without leaving any remains on the ground.

4.1 Path planning

As in Fig. 4 we assume that the reclaimer can dig down as much as $R\cos\ \phi$ with one slew of the boom. Recall that R is the radius of the rotating disk, and ϕ is the tilt angle of the disk against the vertical plane in the 4th link coordinate frame. The solid lines $h_i = i(\text{R}\cos\ \phi)$, $i = 1,\ 2,\ \ldots,$ indicate the ith slew level from the ground along which the bottom tip of the disk will cut through. Therefore, if the center of the disk reaches the height h_i, then the complete removal of raw materials can be accomplished. The main objective of this section is to determine the initial landing point $(x_0,\ y_0,\ z_0)_i$ at each slew level.

Define $\triangle h_i = x_{0i} - h_i$, where x_{0i} is the x-component of the initial excavation point at the ith level.

4.2 Calculation of $\triangle h_i$

We first evaluate $\triangle h_i$ at each slew level. If the profile of a raw materials heap is irregular, then $\triangle h_i$ will be different at each level and has to be determined at each slew level. However, if the shape of the raw materials pile is uniform and the overall shape differs only depending on the kind of raw materials, then $\triangle h_i = \triangle h$, $i = 1,\ 2,\ \cdots,\ n$, can be asserted. In this paper we assume that the pile is regular and the slope is uniform. Hence θ_m
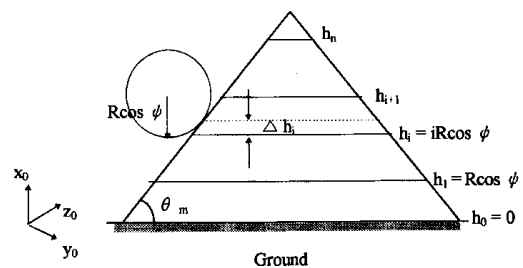

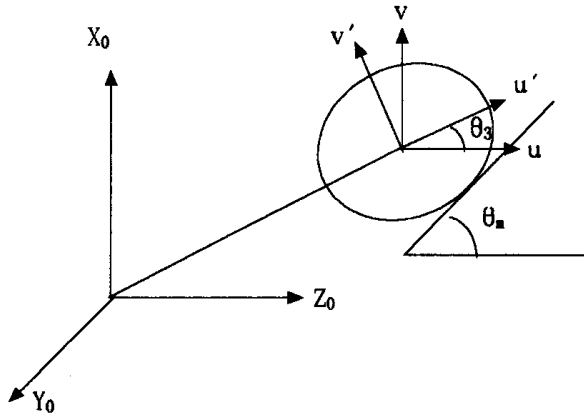**Fig. 4** Slewing levels of boom

Fig. 5 Lateral view of the disk projected along the z_2-axis

in Fig. 4 is a constant which can be decided once the type of material is given.

Figure 5 shows a side view of the rotating disk which contacts an excavation point. The center of view point is the origin of the 5th coordinate frame and the view direction is parallel to the axis of z_2. The uv-plane in Fig. 5 is a vertical plane whose origin is centered at the origin of the 5th link coordinate system. The u-axis and v-axis are parallel to the ground and x_0-axis in Fig. 2, respectively. The u'v'-coordinate system indicates the rotation of the uv-coordinate system by θ_3. Since the disk tilts as much as φ and ϕ, the projected shape of the disk to the u'v'-plane becomes an ellipse. Now the equation of the ellipse in the u'v'-coordinate system becomes

$$\frac{u'^2}{(R\cos \phi)^2} + \frac{v'^2}{(R\cos \psi)^2} = 1 \qquad (5)$$

Also, since the u'v'-coordinate has rotated by θ_3, the following transformation between the uv-coordinate and u'v'-coordinate holds:

$$\begin{bmatrix} u' \\ v' \end{bmatrix} = \begin{bmatrix} \cos \theta_3 & \sin \theta_3 \\ -\sin \theta_3 & \cos \theta_3 \end{bmatrix} \begin{bmatrix} u \\ v \end{bmatrix} \qquad (6)$$

Therefore, the equation of the ellipse in the uv-coordinate system becomes

$$\frac{(\cos \theta_3 u + \sin \theta_3 v)^2}{(R\cos \phi)^2} + \frac{(-\sin \theta_3 u + \cos \theta_3 v)^2}{(R\cos \psi)^2}$$
$$= 1 \qquad (7)$$

On the other hand when the boom slews horizontally, the maximum load occurs at the point where the raw materials protrude out most toward the reclaimer. The intersection between the uv-plane and the ore pile is a line and can be written as

$$v = \tan \theta_m u + \eta \qquad (8)$$

where η is the intercept on the v-axis. Substituting (8) into (7), the resulting equation becomes an equation of only u and η. Since we are interested in the case when the ellipse contacts the line, the determinant term of the quadratic equation of u, which involves η, must be zero. Hence the value of η is determined. Therefore, a unique of u is now determined. Finally substituting u and η into (8), v is obtained. The results are summarized as follows:

$$u = \frac{-\eta\{ (R\cos \psi)^2(\cos \theta_3 + \sin \theta_3\tan \theta_m)\sin \theta_3 + (R\cos \phi)^2(\cos \theta_3\tan \theta_m - \sin \theta_3)\cos \theta_3 \}}{\{ (R\cos \phi)^2(\cos \theta_3 + \sin \theta_3\tan \theta_3)^2 + (R\cos \phi)^2(\cos \theta_3\tan \theta_m - \sin \theta_3)^2 \}}$$
$$v = \tan \theta_m u + \eta \qquad (9)$$

where

$$\eta = -\frac{\sqrt{Q}(R\cos \phi)(R\cos \psi)}{\sqrt{Q(R\cos \psi)^2\sin^2 \theta_3 + Q(R\cos \phi)^2\cos^2 \theta_3 - P}}$$

$$P = (R\cos \psi)^2(\cos \theta_3 + \sin \theta_3\tan \theta_m)\sin \theta_3$$
$$+ (R\cos \phi)^2(\cos \theta_3\tan \theta_m - \sin \theta_3)\cos \theta_3$$

$$Q = (R \cos \psi)^2(\cos \theta_3 + \sin \theta_3 \tan \theta_m)^2 + (R \cos \phi)^2$$
$$(\cos \theta_3\tan \theta_m - \sin \theta_3)^2$$

Now if the center of the rotating disk is located at the level h_{i+1}, which implies that the origin of the uv-coordinate system is located at h_{i+1}, then

$$\Delta h_i = h_{i+1} - h_i - | v |.$$

Since Δh_i is obtained at each level, the x_o-component of the initial excavation point at each level is determined in the reference coordinate system.

4.3 A closed-form solution

With the x_0-component of the initial digging point obtained in Sec. 4.2, we assume that y_0, z_0 are provided from the excavation point determi-

nation algorithm. Now consider the transformation matrix between the 3rd coordinate frame and 5th coordinate frame to incorporate the inclination of the rotating drum from the boom. The position vector O of the center of the drum in the 5th coordinate frame can be converted to a vector in the 3rd coordinate frame as follows:

$$^3P = {}^3T_4 {}^4T_5 {}^5P$$

$$= \begin{bmatrix} \sin\phi & 0 & \cos\phi & 0 \\ -\cos\phi & 0 & \sin\phi & 0 \\ 0 & -1 & 0 & d_4 \\ 0 & 0 & 0 & 1 \end{bmatrix} \begin{bmatrix} -\sin\psi & 0 & \cos\psi & 0 \\ \cos\psi & 0 & \sin\psi & 0 \\ 0 & 1 & 0 & 0 \\ 0 & 0 & 0 & 1 \end{bmatrix} \begin{bmatrix} 0 \\ 0 \\ d_6 \\ 1 \end{bmatrix}$$

$$= \begin{bmatrix} d_6\sin\phi\cos\psi \\ -d_6\cos\phi\cos\psi \\ -d_6\sin\psi + d_4 \\ 1 \end{bmatrix} \qquad (10)$$

where ^3P denotes the vector of the center of the drum in the 3rd coordinate frame. Now by using the geometry in Fig. 6 with Eq. (10) the values of points O, O_2 and O' are obtained in the 2nd coordinate frame as follows.

$$O = (a_3 + d_6\sin\phi\cos\psi, \quad -d_6\sin\psi + d_4,$$
$$d_6\cos\psi\cos\phi)$$
$$O_2' = (0, 0, d_6\cos\phi\cos\psi)$$
$$O' = (a_3 + d_6\sin\phi\cos\psi, \quad d_6\cos\phi\cos\psi)$$

where O_2' denotes the translation of the origin of the 2nd coordinate frame to the direction of the z_2 -axis by $d_6\cos\phi\cos\psi$. O' refers to the projection of O on the $x_2 z_2$ plane. The upper portion in Fig. 6 shows the projected coordinate frames of the boom on the $y_0 z_0$ plane (ground), and the lower portion in Fig. 6 indicates the z_2-axis (The shape of the drum needs to be an ellipse).

The joint variable θ_3 can now be calculated from the geometry as in Fig. 6 as follows:

$$\theta_3 = \beta - \alpha = \text{atan2}(\sin\beta, \sqrt{1-\sin^2\beta})$$
$$- \text{atan2}(-d_6\sin\psi + d_4, \ a_3$$
$$+ d_6\sin\phi\cos\psi) \qquad (11)$$

where

$$\sin\beta = \frac{h - d_2}{\sqrt{(a_3 + d_6\sin\phi\cos\psi)^2 + (d_6\sin\psi + d_4)^2}}$$

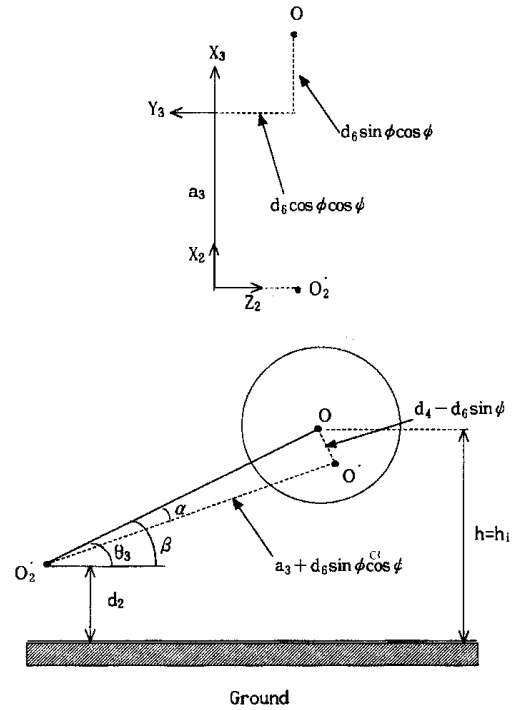Finally, from the forward kinematics Eqs. (2) ~ (4), a closed form inverse kinematics solution is obtained as

Fig. 6 Geometry for obtaining θ_3

$$\theta_r = \text{atan2}(B, A) \pm \text{atan2}(x_0 - C,$$
$$\sqrt{A^2 + B^2 - (x_0 - C)^2}) \qquad (12)$$
$$\theta_2 = -\text{atan2}(E, D) \pm \text{atan2}(\sqrt{D^2 + E^2 - y_0^2}, \ y_0) \quad (13)$$
$$d_1 = z_0 - \cos\theta_2[\cos\theta_3\{a_6\cos\phi\sin\theta_r + \sin\phi(d_6\cos\psi - a_6$$
$$\sin\psi\cos\theta_r)\}$$
$$- \sin\theta_3(-a_6\cos\phi\cos\theta_r - d_6\sin\psi + d_4) + a_3\cos\theta_3]$$
$$+ \sin\theta_2\{\cos\phi(d_6\cos\psi - a_6\sin\psi\cos\theta_r)$$
$$- a_6\sin\phi\sin\theta_r\} \qquad (14)$$

where

$$A = a_6\sin\theta_3\cos\phi$$
$$B = a_6(\sin\phi\sin\psi\sin\theta_3 + \cos\psi\cos\theta_3)$$
$$C = d_6\sin\phi\cos\psi\sin\theta_3 - d_6\sin\psi\cos\theta_3$$
$$+ d_4\cos\theta_3 + a_3\sin\theta_3 + d_2$$
$$D = \cos\phi(d_6\cos\psi - a_6\sin\psi\cos\theta_r)$$
$$- a_6\sin\phi\sin\theta_r$$
$$E = \cos\theta_3\{a_6\cos\phi\sin\theta_r + \sin\phi(d_6\cos\psi$$
$$- a_6\sin\psi\cos\theta_r)\}$$
$$+ \sin\theta_3(a_6\cos\psi\cos\theta_r + d_6\sin\psi$$
$$- d_4) + a_3\cos\theta_3$$

5. Inverse Kinematics (Approach #2)

In this section we investigate the inverse kinematics problem for a given arbitrary excavation point in space.

5.1 Derivation of a plane equation

As was seen from Eqs. (2) ~ (4), the number of joint variables is one greater than the number of equations. Therefore, one more equation is necessary in order to acquire a closed-form inverse kinematics solution. In this paper we exploit an extra equation using the fact that the circle connecting the tips of buckets should contact the surface of the bulk.

First we derive a plane equation which approximates the surface around the excavation point. This is because it is not possible to obtain an exact surface equation for the whole bulk. Therefore, it is reasonable to approximate the area near the excavation point as a plane. The plane equation can be obtained by the least squares method by utilizing 8 adjacent points near the excavation point. Let the normal vector at the excavation point be $\hat{n} = (n_x, n_y, n_z)$. Then the plane equation can be written as

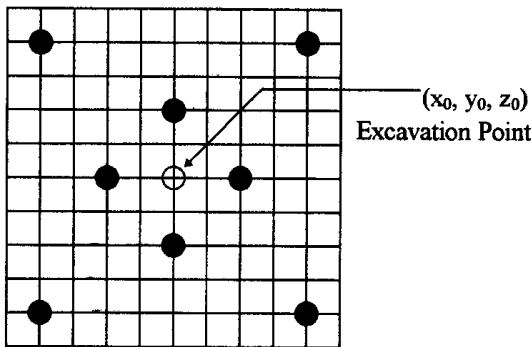$$n_x \cdot x + n_y \cdot y + n_z \cdot z = 1 \qquad (15)$$

Substituting 9 points as in Fig. 7 into (15) yields a matrix equation as follows:

$$\begin{bmatrix} x_0 & y_0 & x_0 \\ \cdot & \cdot & \cdot \\ \cdot & \cdot & \cdot \\ \cdot & \cdot & \cdot \\ x_8 & y_8 & z_8 \end{bmatrix} \begin{bmatrix} n_x \\ n_y \\ n_z \end{bmatrix} = \begin{bmatrix} 1 \\ \cdot \\ \cdot \\ \cdot \\ 1 \end{bmatrix} \qquad (16)$$

In a simplified form

$$W \cdot \hat{n} = u$$

where W is a 9×3 matrix, $\hat{n}$ is a normal vector, and u is a column vector with all element equal

to 1. The column/row vectors of W are independent, and therefore $W^T W$ is a symmetric square matrix and its inverse exists (Strang, 1988). Hence the normal vector $\hat{n}$ can be obtained as a solution to the normal equation as follows (Luenberger, 1969):

$$\hat{n} = (W^T W)^{-1} W^T u \qquad (17)$$

5.2 Constraint equation and linear approximation

Since the information about the profile of the bulk is now incorporated in Eq. (17), we utilize the fact that the circle connecting the tips of buckets should contact the plane. As is shown in Fig. 8, the z_6-axis of the 6th joint coordinate system should be perpendicular to the normal vector. The following constraint equation is obtained:

$$\begin{aligned} &n_y[\cos \theta_2(\cos \phi \sin \psi \sin \theta_r - \sin \phi \cos \theta_r) \\ &- \sin \theta_2\{\cos \theta_3 \cdot (\sin \phi \sin \psi \sin \theta_r + \cos \phi \\ &\cos \theta_r) - \cos \psi \sin \theta_3 \sin \theta_r \}] \\ &+ n_z \cdot [\cos \theta_2\{\cos \theta_3(\sin \phi \sin \psi \sin \theta_r \\ &+ \cos \phi \cos \theta_r) \\ &- \cos \psi \sin \theta_3 \sin \theta_r \} + \sin \theta_2(\cos \phi \sin \psi \\ &\sin \theta_r - \sin \phi \cos \theta_r)] \\ &+ n_x[\sin \theta_3 \cdot (\sin \phi \sin \psi \sin \theta_r + \cos \phi \\ &\cos \theta_r) + \cos \psi \cos \theta_3 \sin \theta_r] = 0 \qquad (18) \end{aligned}$$

The forward kinematics Eqs. (2) ~ (4) and the constraint Eq. (18) allow the analysis of inverse kinematics. However, it is impossible to obtain a closed form solution from the above 4 equations since they involve trigonometric functions and are highly nonlinear. In this section we propose instead an approximate solution using

Fig. 7 Selected 8 adjacent points for the least square approximation
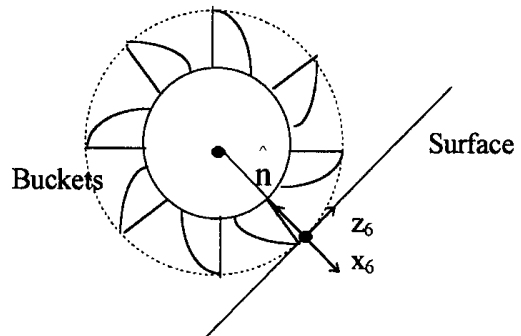
Fig. 8 Orthogonality between z_6-axis and $\hat{n}$

the Newton-Raphson method. Let us rewrite (2) ~ (4) and (18) as follows:

$$x_0 = f_1(d_1,\ \theta_2,\ \theta_3,\ \theta_r)$$
$$y_0 = f_2(d_1,\ \theta_2,\ \theta_3,\ \theta_r)$$
$$z_0 = f_3(d_1,\ \theta_2,\ \theta_3,\ \theta_r)$$
$$0 = f_4(d_1,\ \theta_2,\ \theta_3,\ \theta_r) \tag{19}$$

We expand (19) at some initial conjectured estimate as $\Theta_0 = [d_1^0,\ \theta_2^0,\ \theta_3^0,\ \theta_r^0]^T$, and eliminate higher terms beyond the linear term. Hence we have

$$\begin{bmatrix} x_0 \\ y_0 \\ z_0 \\ 0 \end{bmatrix} = \begin{bmatrix} f_1 \\ f_2 \\ f_3 \\ f_4 \end{bmatrix}_{\Theta_0} + \begin{bmatrix} \dfrac{\partial f_1}{\partial d_1} & \dfrac{\partial f_1}{\partial \theta_2} & \dfrac{\partial f_1}{\partial \theta_3} & \dfrac{\partial f_1}{\partial \theta_r} \\[2mm] \dfrac{\partial f_2}{\partial d_1} & \dfrac{\partial f_2}{\partial \theta_2} & \dfrac{\partial f_2}{\partial \theta_3} & \dfrac{\partial f_2}{\partial \theta_r} \\[2mm] \dfrac{\partial f_3}{\partial d_1} & \dfrac{\partial f_3}{\partial \theta_2} & \dfrac{\partial f_3}{\partial \theta_3} & \dfrac{\partial f_3}{\partial \theta_r} \\[2mm] \dfrac{\partial f_4}{\partial d_1} & \dfrac{\partial f_4}{\partial \theta_2} & \dfrac{\partial f_4}{\partial \theta_3} & \dfrac{\partial f_4}{\partial \theta_r} \end{bmatrix}_{\Theta_0} \begin{bmatrix} \triangle d_1 \\ \triangle \theta_2 \\ \triangle \theta_3 \\ \triangle \theta_r \end{bmatrix} \tag{20}$$

In abbreviated form

$$X = f(\Theta_0) + J(\Theta_0)\,\Delta\Theta \tag{21}$$

where $X = [x_0,\ y_0,\ z_0,\ 0]^T$ represents a desired end-effector location. Therefore

$$\Delta\Theta = J^{-1}(\Theta_0)\,(X - f(\Theta_0)) \tag{22}$$

Recursively updating the estimate Θ within a given error bound, a better approximation can be obtained as follows (Press et al., 1987):

$$\Delta\Theta_{i+1} = J^{-1}(\Theta_i)\,(X - f(\Theta_i)),\quad i = 0,\ 1,\ 2,$$
$$\Theta_{i+1} = \Theta_i + \triangle\Theta_{i+1}$$
If $\|\Delta\Theta_{i+1}\| \le \varepsilon$, then stop. $\tag{23}$

6. Comparison

We compare two solutions obtained through the two approaches in Sec. 4 and 5 by simulations and graphical representation. Figure 9 shows the 3-dimensional profile of an iron ore scanned through by a laser sensor. Its 2-dimensional contours projected to the ground are shown in Fig. 10. The following parameters are used for numerical computations: $d_2 = 9,500$ mm, $a_3 = 46,100$ mm, $d_4 = 1,100$ mm, $d_6 = 1,226.8$ mm, $a_6 = 2,800$ mm, $\varphi = 2°$, $\psi = -12°$. The inverse kinematics solutions for the two methods for a desired landing point on the contour of a level 800 mm high are tabulated below. Since the inverse kinematics solution using the first approach is closed-form, the forward kinematics solution will provide the exact same excavation
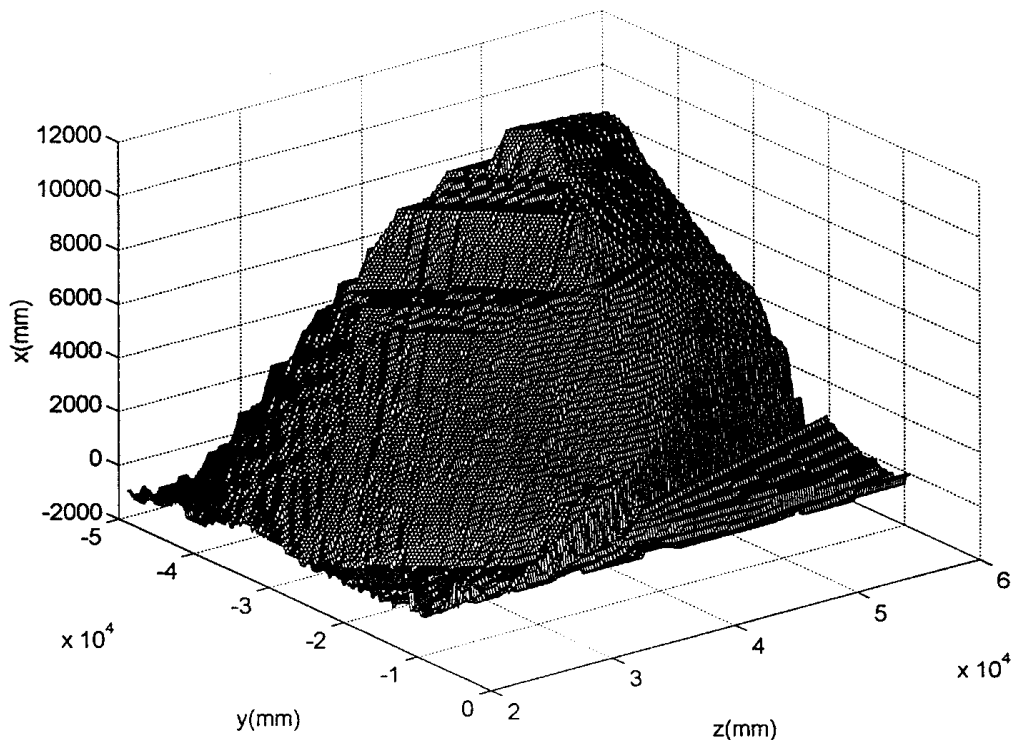

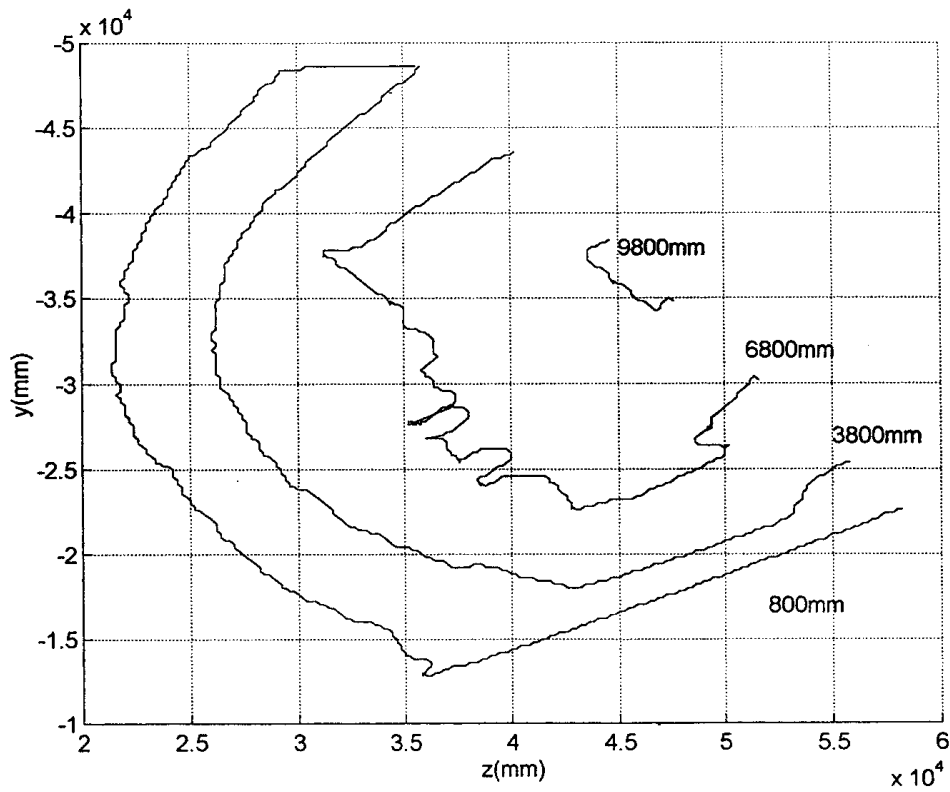**Fig. 9** 3-Dimensional profile of an iron ore heap

Fig. 10 2-Dimensional projected contours of the iron ore heap in Fig. 9 (y_0-z_0 plane)
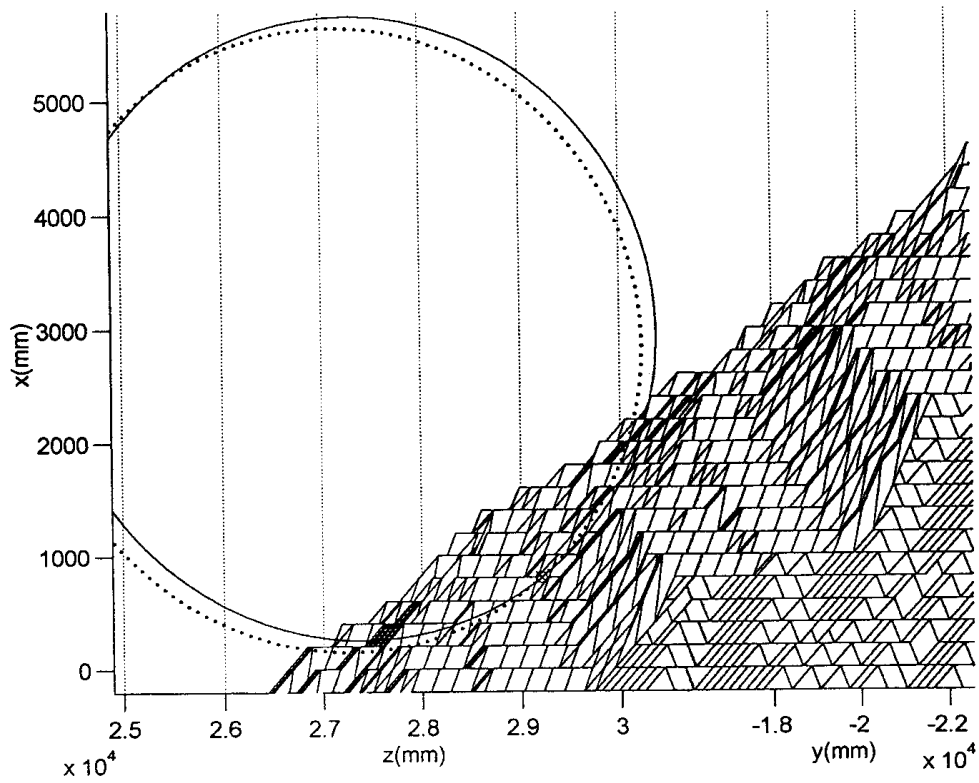

Fig. 11 View of the two rotating disks contacting an ore heap in Fig. 9
(View direction $(x, y, z) = (0, -1, -0.44)$)

point. On the other hand the second approach   may yield some numerical error. It is remarked

Table 1 Given excavation point (800, −19545, 27898) mm

Variables	Inverse Kinematics				Forward Kinematics to O_5		
	d_1 (mm)	θ_2 (rad)	θ_3 (rad)	θ_r (rad)	x (mm)	y (mm)	z (mm)
Method 1	−15316.0	0.457	−0.171	0.816	2998.3	−19088.0	26226.0
Method 2	−15444.0	0.455	−0.173	0.979	2893.4	−19004.0	26119.0

that the location of the drum circumference in the bulk is as important as getting near the given excavation point, since an irregular material pile may cause the system to overload. Hence, the forward kinematics solutions have been obtained for the center of the drum instead of the excavation point. If the given material profile is regular, not much difference is found. However, the second approach yields much more uneven results compared to the first approach. This is due to the fact that the second method utilizes the normal vector at each point, which is highly location dependent. Figure 11 shows the side view of the disks contacting the surface. In Fig. 11, × denotes the location of an excavation point, and ○ indicates the forward kinematics solutions by both approaches 1 and 2. The solid big circle indicates the location of the disk obtained by approach 1, and the dotted circle shows the location of the disk obtained by approach 2. The authors recommend the first approach for a real application in the storage yard.

7. Conclusions

In this paper the inverse kinematics problem of obtaining joint variables of a reclaimer has been investigated for the first time. For a desired end-effector location in space the forward kinematics provide 3 equations. However, the number of

involved joint variables is 4, yielding kinematic redundancy. Two approaches are investigated for the solution of the inverse kinematics. The first approach assumes knowledge of the drum height while slewing, and then determines the remaining joint variables from the forward kinematics equations. A closed-form solution is obtained for the first approach. The second approach is based on the geometric constraint that the excavating bucket must contact the surface of the bulk. A closed-form solution is not found for the second approach. Instead an approximate solution to the nonlinear inverse problem is suggested.

References

Fu, K. S., Gonzalez, R. C. and Lee, C. S. G., 1987, *Robotics*, McGraw-Hill, New York.

Luenberger, D. G., 1969, *Optimization by Vector Space Methods*, John Wiley & Sons, Inc. New York.

Press, W. H., Teukolsky, S. A., Vetterling, W. T. and Flannery, B. P., 1992, *Numerical Recipes*, Cambridge University Press.

Sandor, G. N. and Erdman, A. G., 1984, *Advanced Mechanism Design: Analysis and Synthesis*, Vol. 2, Prentice Hall, Englewood Cliffs, NJ.

Strang, G., 1988, *Linear Algebra and Its Applications*, Harcourt Brace Jovanovich, Inc.